

# Characterization and Implementation of a Vision-Based 6-DOF Localization System

James Doebbler\*, Jeremy J. Davis\*, John Valasek<sup>†</sup>, John L. Junkins<sup>‡</sup>

*Aerospace Engineering Dept, Texas A&M University, College Station, TX 77840-3141*

Testing and validation of flight hardware in ground-based facilities can result in significant cost savings and risk reduction. We focus particular attention on ground validation for small satellite proximity operations. We designed a relative motion emulation system for aerospace vehicles using Relative Motion Vehicles (RMVs) capable of large planar motion and limited 6 degree-of-freedom motion. Though the state of the RMV is approximated through internal sensors, an external measurement system is required to correct for secular drift. The commercial NorthStar system from Evolution Robotics provides a vision-based 2-D localization solution using active infrared (IR) beacons. This paper addresses characterization and implementation of the NorthStar system as a 6-DOF state measurement system. The noise characteristics of the NorthStar Detector were determined, as were the output characteristics of the IR light emitting diode (LED) beacons. These characteristics were used to produce a high fidelity model of the measurement system in which multiple Detectors are placed around the perimeter of the workspace and multiple beacons are installed on the RMV. Simulation and hardware test results demonstrate the efficacy of this approach.

## Nomenclature

$\mathbf{X}$	Inertial frame position vector
$\boldsymbol{\sigma}$	Modified Rodrigues Parameters (MRP) relating a given frame to the inertial frame
$\mathbf{x}$	Unknown 6-D state vector
$\mathbf{b}_i$	Line of sight measurement vector to beacon $i$ in the detector frame
$\mathbf{r}_i$	Line of sight measurement vector to beacon $i$ in the inertial frame
$r_i$	Magnitude of $\mathbf{r}_i$
$W$	Positive definite weighting matrix for GLSDC
$H$	Measurement Jacobian matrix
$[A]$	Direction cosine matrix mapping inertial into detector frame
$[C]$	Direction cosine matrix mapping inertial frame into RMV frame
$[I_{3 \times 3}]$	$3 \times 3$ identity matrix

### Subscript

$d$	NorthStar Detector
$r$	Relative Motion Vehicle (RMV)
$i$	Beacon index

## I. Introduction

MULTI-VEHICLE proximity operations of spacecraft, from formation flying to automated rendezvous and docking, represent an active area of current research with many obvious benefits. Ground-based testing of the autonomous control algorithms for multiple vehicles with sensors or docking hardware in-the-loop provides significant risk reduction for such missions. We are developing a relative motion emulation system based on multiple mobile platforms,

\*Graduate Research Assistant, Student Member AIAA.

<sup>†</sup>Professor and Director, Flight Simulation Laboratory, Associate Fellow AIAA.

<sup>‡</sup>Distinguished Professor, Fellow AIAA.

termed Relative Motion Vehicles (RMVs). The payload of the RMV will be the sensor, docking hardware, or full vehicle being tested, and the RMV will track the motion specified by a high fidelity dynamic model of that payload.

The mobile platform approach provides several distinct advantages over existing facilities such as NRL's Proximity Operations Testbed<sup>1</sup> and NASA's Flight Robotics Facility:<sup>2</sup>

1. Allows for un-tethered circumnavigation of two or more vehicles;
2. Mobile nature enables testing or demonstration at any location with a large enough workspace;
3. Low-cost alternative to larger installations while maintaining high fidelity; and
4. Supports testing of non-spacecraft multi-vehicle systems, such as autonomous aerial refueling.

To enable high-fidelity motion emulation, significant effort has been made toward modeling the dynamics and control of the RMV and developing the internal sensing systems.<sup>3-5</sup> The first generation RMV primarily relies on integrating wheel motion to obtain a position estimate, a process known as odometry. Future generations will employ an inertial measurement unit (IMU) to further augment the internal sensing.

Regardless of the accuracy achieved through these methods, internal sensing systems drift over time (IMU) or distance traveled (odometry), so some form of external inertial measurement system is required. On orbit, conventional sensors such as star sensors, GPS, or other inertial navigation can be used. However, for indoor laboratories alternative navigation technologies are required. Many different sensing systems exist, but to enable the advantages of this facility listed above, certain criteria must be met. First, a portable system that can be moved from location to location is needed to enable testing at various facilities. Second, one major advantage is the ability to accommodate more than two vehicles, so the system must be extensible to large numbers of vehicles. Third, the measurement system must be able to accurately measure across a large distance, as the anticipated workspace of this facility is several hundred square feet. Lastly, we desire to find an inexpensive, commercial solution.

The long range accuracy requirement discounts sonar sensors as a possibility, whereas the portability requirement precludes ceiling-mounted cameras or sensors embedded in the floor. Additionally, most vision based sensors are extremely sensitive to the environment, particularly lighting conditions, and are thus ill-suited for a portable facility. Commercial laser based solutions such as iGPS or laser trackers provide extremely high accuracy at large distances, but cost tens to hundreds of thousands of dollars.

Evolution Robotics, the makers of the vision system used by Sony's Aibo, has recently developed the NorthStar Developer's Bundle for use as a low-cost mobile robot localization device. The kit consists of two Projectors that project infrared light spots on the ceiling, and a Detector that outputs the centroid locations of the spots in detector coordinates in addition to the planar pose (position and orientation) estimate that it can compute once calibrated for ceiling height. The lenses of the Projectors can also be removed to allow for direct view of the IR emitters in a beacon mode.

We have used this direct beacon mode to produce a 6-D state estimate of our mobile robot. A detailed description of the NorthStar sensing system is found in Section II. We have conducted detailed characterization of the NorthStar system in beacon mode, presented in Section III. Section IV describes the use of this system as a 6-DOF measurement system and presents results from simulation tests.

## II. NorthStar and VisNav Systems

The NorthStar system provides a vision-based localization solution.<sup>6,7</sup> Whereas many vision-based sensors suffer from sensitivity to the environment, NorthStar overcomes this by using structured infrared light. Typical light sources have little impact, as the NorthStar Detector is optimized for 950nm wavelength light. Additionally, the light from the NorthStar Projectors or beacons is modulated at frequencies between 1kHz-3kHz to further distinguish itself from any ambient noise. Each beacon is modulated at a unique frequency, and the Detector is capable of identifying up to 20 unique beacon IDs simultaneously at an update rate of about 10Hz. The Detector is extremely small, measuring only 4.00cm × 3.60cm × 1.05cm, though Evolution Robotics recommends a thin protective window be placed over it to prevent damage from impact or electro-static discharge.<sup>8</sup>

The Projectors consist of a cluster of four IR LEDs pointing in a common direction and a removable Fresnel lens to project spots on the ceiling. By viewing the light spots reflected off a diffusely-reflecting ceiling, and assuming the Detector is flat and level, a 2-D position and orientation pose estimate is obtained. Noise characteristics of the NorthStar system in this mode are detailed in documentation available from NorthStar.<sup>8</sup> Though localization within

1cm-4cm is possible, this method depends on a low, flat, diffusely-reflecting ceiling and most energy is lost rather than reflected off the ceiling towards the Detector.

To counteract these issues, the LEDs may be viewed directly by the Detector by removing the Fresnel lens. Evolution Robotics recommends mounting the Detector to the ceiling and placing these IR beacons on the mobile asset to be tracked. The only sensor noise information provided about this mode is that position errors lie within 15cm ( $1-\sigma$ ) for a 6m ceiling.<sup>8</sup> Detailed characterization of the Detector in beacon mode is provided in the next section.

To utilize NorthStar as a 6-DOF localization system, we look to the VisNav sensor, another vision-based sensor that utilizes active IR beacons.<sup>9-11</sup> A position-sensing diode (PSD) provides line of sight measurements to each beacon sequentially. Two-way communication between the PSD and the beacons allows the PSD to toggle each beacon on and off and command varying intensity to maximize the signal-to-noise ratio while avoiding sensor saturation.

In the VisNav setup, beacons are placed in known locations with respect to a target frame, and by sampling each beacon a full 6-DOF state of the PSD relative to the target can be produced at 100Hz. The set of measurements is run through a Gaussian Least-Squares Differential-Correction (GLSDC) algorithm to estimate the 6-DOF state.

The NorthStar Detector can be used in place of the PSD and includes the capability of sampling all beacons within its field of view simultaneously. Given the beacon locations fixed in an inertial frame, the position and orientation of a Detector fixed to an RMV can be obtained. Conversely, Detectors fixed in an inertial frame can provide a 6-DOF estimate of a group of beacons fixed in an RMV frame. This latter method is adopted as the preferred approach in this paper, as it allows additional RMVs to be added for the cost of several inexpensive LED beacons rather than additional NorthStar Detectors. An analogous setup would be feasible for the VisNav sensor; we leave this for future studies.

### III. NorthStar Characterization in Beacon Mode

Documentation available from Evolution Robotics provides detailed characterization of the system when used to provide planar pose estimates from spots projected on the ceiling. A detailed characterization of the NorthStar system in beacon mode is necessary for accurate modeling of the 6-DOF state measurement system. We used these models to design an effective localization method.

#### A. Detector

To complete the characterization of the NorthStar Detector, its outputs were sampled in a variety of situations. The Detector outputs beacon locations in non-dimensional detector coordinates with a range of  $\pm 32,768$  as well as a non-dimensional measured intensity between 0 and 65,535.

We first placed a NorthStar Beacon at distances between 2.7ft and 60ft along the boresight of the Detector and recorded 1000 samples at each step. Data was taken using 1, 2 and 4 LEDs illuminated. The Beacon saturated the Detector and produced inaccurate results when closer than 18ft for the 4 LED case, 13ft for the 2 LED case, and 8ft for the 1 LED case. These data points were discarded in the subsequent analysis, although the saturation conditions were noted for later consideration. Ambient noise intensity values ranged between 50 and 150 in an indoor hallway with overhead fluorescent lights.

As expected, we found that the measured light intensity scales linearly with the number of LEDs illuminated. Given this relationship, we scaled the data down to the intensity given by a single LED to characterize the noise of the Detector. Figure 1 shows the single standard deviation noise as a function of measured light intensity. Modeling this relationship as noise inversely proportional to intensity shows close agreement with the data as shown by a least squares fit of the data.

The second test conducted was to rotate the Detector by  $5^\circ$  increments up to  $\pm 60^\circ$  off boresight (the specified field of view of the Detector) while the beacon was held fixed. There existed a strong relationship between this incidence angle and the intensity as measured by the Detector, as shown in Fig. 2. The relationship was symmetric about  $0^\circ$ , so a second order polynomial was fit by averaging the values of measurements the same distance of boresight (ie. intensity values for  $5^\circ$  and  $-5^\circ$  were averaged).

Viewing the raw data acquired during the angles test revealed that the 1,000 data points for a given angle took the shape of an ellipse when the beacon was off boresight. As Fig. 3 shows, this uncertainty ellipse has its major axis along the radial direction from boresight, such that the angle of the major axis of the ellipse is equal to the azimuth angle of the centroid location. Fitting a 2-D Gaussian distribution to each of these ellipses, we found that out of the 75,000 data points collected over 75 ellipses, 39.3% of those data points fell within the  $1-\sigma$  ellipse defined by the Gaussian fit, whereas 86.5% fell within  $2-\sigma$  and 98.9% within  $3-\sigma$ . Compared to the theoretical values of the confidence intervals for Gaussian noise of 39.4% ( $1-\sigma$ ), 86.5% ( $2-\sigma$ ), and 98.9% ( $3-\sigma$ ), this near perfect match

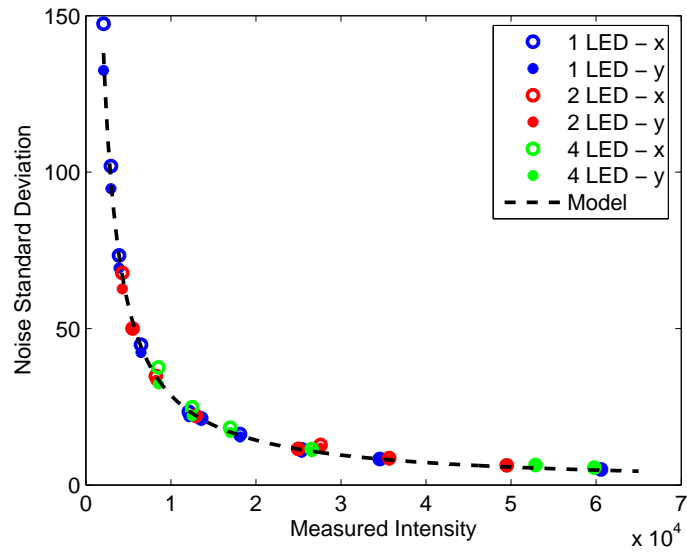


Figure 1. Standard deviation noise as a function of measured intensity. Least squares fitting shows an inversely proportional relationship.

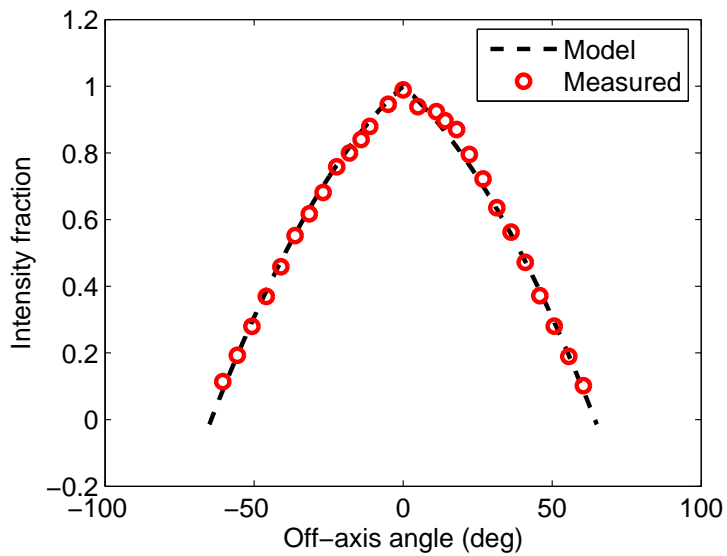
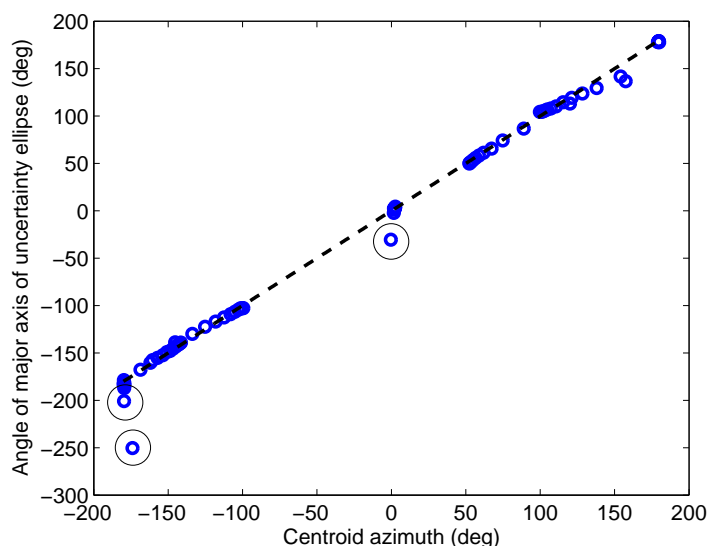


Figure 2. Measured intensity versus the incidence angle on the detector. Least-squares fitting of a symmetric second order relationship shown.

validates the typical assumption that the noise has a Gaussian distribution.



**Figure 3. Angle of major axis of uncertainty ellipse versus centroid azimuth angle. The line with unit slope shows one-to-one correlation. The three outliers (circled) correspond to points closest to boresight with poorly determined major and minor axes.**

The model for the size of the  $1\text{-}\sigma$  ellipse was defined as follows. Given the measured intensity from the Detector, a reference value for the noise can be found from the relationship shown in Fig. 1. Although this noise value is only valid when the centroid is located along the boresight of the Detector, it can be scaled by two factors dependent on the distance off boresight to find the two dimensions of the  $1\text{-}\sigma$  ellipse. Visual inspection of the magnitudes of the major and minor axes compared to this reference noise value led to a scaling factor between them based on sines and cosines of the normal distance,  $d$ , of the centroid from boresight. The reference noise value was scaled by a factor of  $\cos\left(\frac{\pi}{2} \frac{d}{d_{max}}\right)$ , where  $d_{max} = 32,768$ , to determine the semi-minor axis, whereas the reference noise value was scaled by a factor of  $1 + 3.47 \sin\left(\pi \frac{d}{d_{max}}\right)$  to determine the semi-major axis. As desired, these scalings map the ellipse to a circle when it is on boresight (ie.  $d = 0$ ). To demonstrate this model, the semi-major and minor axes found by fitting Gaussian distributions to the raw data have been scaled by the inverse of these factors to map them back into reference noise values. Figure 4 shows that the scaling factors correctly transform the measured ellipses into the noise model from Fig. 1.

In addition to the relationship between incidence angle and measured intensity, the NorthStar documentation indicates that non-linearities exist in the centroided beacon positions as the beacon moves off the boresight of the Detector. These non-linearities must be accounted for through rigorous calibration of the Detector, but the noise during these tests still correlated with the measured intensity as in the earlier tests.

## B. Beacons

The beacons provided with the NorthStar Projectors utilize four Vishay TSAL7200 IR LEDs. These LEDs have a total radiant power of 35mW and a typical radiant intensity of 60mW/sr when viewed along its center axis.<sup>12</sup> The intensity decreases the further a Detector moves off axis of the LED. The standard metric for assessing the radiation profile of an LED is the half-angle,  $\Phi$ , which measures the off-axis angle where the intensity is half the straight forward intensity. On the TSAL7200s,  $\Phi = 17.5^\circ$ , so the light is focused narrowly. The full radiant intensity profile of the TSAL7200 provided by the datasheet can be approximated by a Gaussian curve, as shown in Fig. 5(a). This intensity profile relates the emission intensity to the angle off-axis the Detector is from a given LED.

Given that the noise correlates to the measured intensity, the TSAL7200 LEDs with only a  $17.5^\circ$  half-angle present a very poor choice for a beacon that can be freely oriented with respect to the Detector. To produce  $360^\circ$  cylindrical coverage of uniform intensity, about 10 LEDs would be needed - and that only supplies the intensity of a single LED. At large distances, an intensity of 4 LEDs (or more) is desired.

Alternatively, the OSRAM SFH4231 Golden Dragon high power IR LED provides 500mW total radiant power

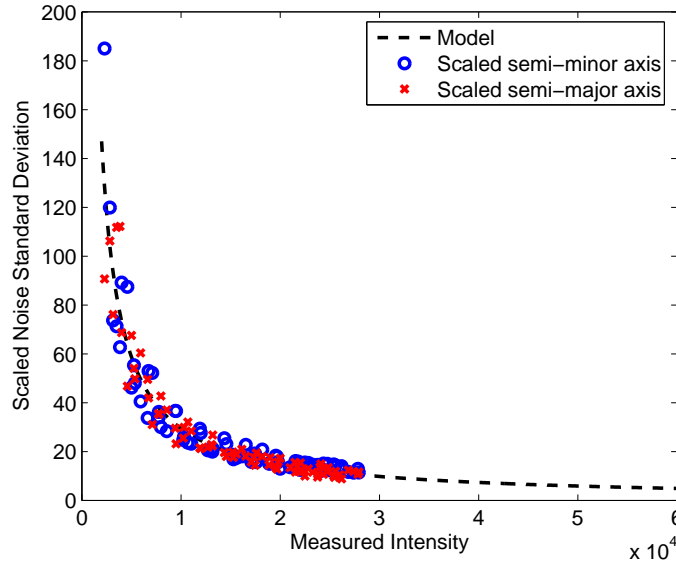


Figure 4. Semi-major and semi-minor axes of the uncertainty ellipse versus measured intensity. The ellipse parameters have been scaled to match the original noise vs intensity model.

with radiant intensity of 200mW/sr and a half-angle of  $60^\circ$ .<sup>13</sup> Viewed along its central axis, a single Golden Dragon provides the intensity of 3.3 TSAL7200 LEDs, and at  $70^\circ$  it provides as much intensity as a single TSAL7200 at  $0^\circ$  as seen in Fig. 5(b). These LEDs were chosen to make the beacons of our localization system.

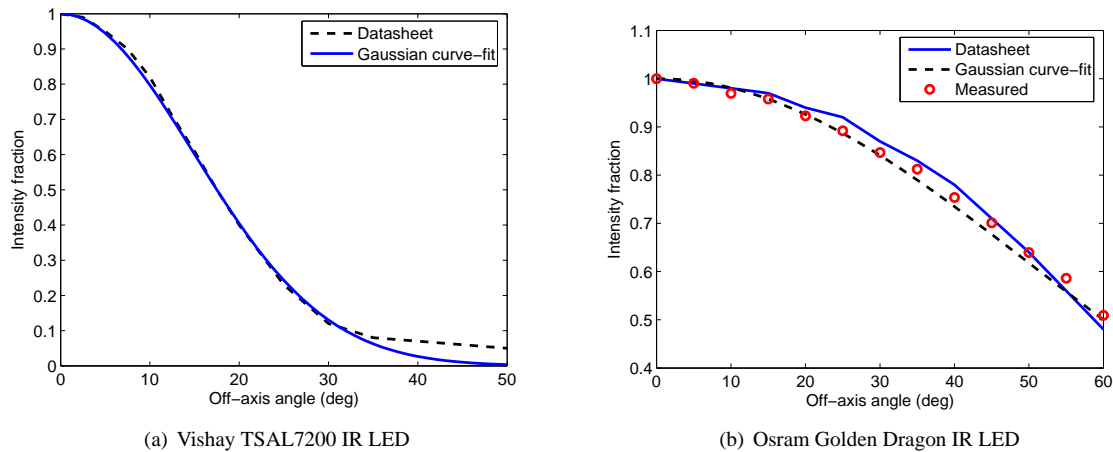


Figure 5. Radiant intensity profile as a function of angle off-axis of an IR LED. Gaussian curves very closely approximate the profiles provided by the datasheets and measured data.

Point light sources exhibit an inverse squared relationship between distance and intensity. The data collected and plotted in Fig. 6 shows that modeling the LED's as point light sources is a valid assumption.

#### IV. Implementation

Several options exist to realize a 6-DOF measurement solution using NorthStar Detectors and beacons. Since we desire a portable facility, the mounting of the Detectors or beacons in the environment should require minimal effort and the required placement accuracy should also be minimized. The significant difference in price between the NorthStar Detector and the beacons led us to distribute multiple beacons on each RMV whereas the Detectors are held

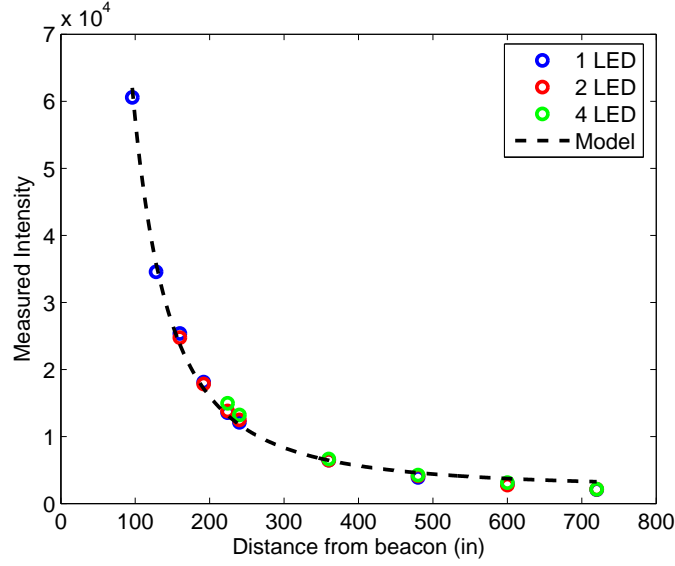


Figure 6. Measured intensity versus the distance from the beacon. Least-squares fitting shows an inverse squared proportional relationship.

fixed in the environment. In this configuration, adding an RMV to the facility requires only the purchase of multiple beacons rather than more Detectors. The Detectors are mounted on collapsible tripods to facilitate easy portability and setup.

### A. Calibration Methodology

The easy portability of Detectors mounted on tripods introduces the challenge that the position and orientation of the Detectors can not be precisely measured. This issue was simply solved by introducing a calibration beacon cluster. The beacon cluster consists of four beacons arranged in a planar square with four OSRAM LEDs per beacon. The beacon cluster is then placed in the center of the workspace, visible to each of the Detectors simultaneously. We define the center of the cluster as the origin (0,0,0) of the inertial frame, whereas each side of the square defines the  $x$  and  $y$  axes with the  $z$  axis defined by the normal to the cluster plane. To compute the 6-DOF state of each Detector, a pinhole camera model is used with GLSDC as is done with VisNav.<sup>9,11</sup> This model and estimation algorithm is described below.

First, we define the collinearity equations for the pinhole camera model. The measurement vector from the Detector to beacon  $i$ , defined in the Detector coordinate frame as  $\mathbf{b}_i$  and in the inertial frame as  $\mathbf{r}_i$ , is defined as:

$$\mathbf{b}_i = \begin{bmatrix} -x_i \\ -y_i \\ f \end{bmatrix}, \quad \mathbf{r}_i = \begin{bmatrix} X_i - X_d \\ Y_i - Y_d \\ Z_i - Z_d \end{bmatrix} \quad (1)$$

where  $(X_i, Y_i, Z_i)$  is the known inertial position of the beacon,  $(X_d, Y_d, Z_d)$  is the unknown Detector position,  $f$  is the focal length, and  $(x_i, y_i)$  are the image coordinates of the measurement. The two vectors relate to each other through the direction cosine matrix,  $[A]$ , such that

$$\hat{\mathbf{b}}_i = [A]\hat{\mathbf{r}}_i \quad (2)$$

where the hat notation indicates normalization of Eq. 1 as unit vectors. We further define  $[A]$  as a function of Modified Rodrigues Parameters (MRPs),<sup>14</sup>  $\boldsymbol{\sigma}_d$ :

$$[A(\boldsymbol{\sigma}_d)] = [I_{3 \times 3}] + \frac{8[\boldsymbol{\sigma}_d \times] - 4(1 - \boldsymbol{\sigma}_d^T \boldsymbol{\sigma}_d)[\boldsymbol{\sigma}_d \times]}{(1 + \boldsymbol{\sigma}_d^T \boldsymbol{\sigma}_d)^2} \quad (3)$$

where the cross operator maps a three element vector into a  $3 \times 3$  matrix as defined by

$$[\mathbf{v} \times] = \begin{bmatrix} 0 & -v_3 & v_2 \\ v_3 & 0 & -v_1 \\ -v_2 & v_1 & 0 \end{bmatrix} \quad (4)$$

The position  $\mathbf{X}_d = (X_d, Y_d, Z_d)$  and orientation  $\boldsymbol{\sigma}_d$  of the Detector comprise the unknown vector  $\mathbf{x}_d$ , whereas the four  $(x_i, y_i)$  pairs from the four beacons provide eight measurements.

The GLSDC algorithm<sup>15</sup> was implemented to solve for the unknowns by minimizing the sum square of the errors

$$J = \frac{1}{2} \sum_i (\hat{\mathbf{b}}_i - \tilde{\mathbf{b}}_i)^T W (\hat{\mathbf{b}}_i - \tilde{\mathbf{b}}_i) = \frac{1}{2} \sum_i \Delta \mathbf{b}_i^T W \Delta \mathbf{b}_i \quad (5)$$

where  $W$  is a diagonal, positive definite, weighting matrix whose elements are the inverse of the covariance of the associated measurement, and  $\tilde{\mathbf{b}}_i = \mathbf{f}(\tilde{\mathbf{x}}_d)$  is the predicted measurement given the estimated state  $\tilde{\mathbf{x}}_d$ . GLSDC an algorithm that iteratively computes a correction to the current estimate based on the Jacobian matrix of the measurement model,  $H = \partial \mathbf{f} / \partial \mathbf{x}_d$ , and the measurement error  $\Delta \mathbf{b}$

$$\Delta \tilde{\mathbf{x}} = (H^T W H)^{-1} H^T W \Delta \mathbf{b} \quad (6)$$

The calculation of the Jacobian can be accomplished by computing the sensitivities for each measurement

$$H_i = \frac{\partial \mathbf{f}}{\partial \mathbf{x}_d} = \begin{bmatrix} \frac{\partial \mathbf{f}}{\partial \mathbf{X}_d} & \frac{\partial \mathbf{f}}{\partial \boldsymbol{\sigma}_d} \end{bmatrix} \quad (7)$$

and vertically stacking them into a single measurement sensitivity matrix

$$H = [H_1^T \ H_2^T \ \dots \ H_N^T]^T \quad (8)$$

given that

$$\mathbf{f}(\tilde{\mathbf{x}}) = [A(\boldsymbol{\sigma}_d)](\mathbf{X}_i - \mathbf{X}_d) / r_i, \quad r_i = \|\mathbf{X}_i - \mathbf{X}_d\| \quad (9)$$

$$\frac{\partial \mathbf{f}}{\partial \mathbf{X}_d} = \frac{1}{r_i} [A(\boldsymbol{\sigma}_d)] (\hat{\mathbf{r}}_i \hat{\mathbf{r}}_i^T - [I_{3 \times 3}]) \quad (10)$$

$$\frac{\partial \mathbf{f}}{\partial \boldsymbol{\sigma}_d} = \frac{4}{(1 + \boldsymbol{\sigma}_d^T \boldsymbol{\sigma}_d)^2} [\mathbf{f} \times] \{ (1 - \boldsymbol{\sigma}_d^T \boldsymbol{\sigma}_d) [I_{3 \times 3}] - 2[\boldsymbol{\sigma}_d \times] + 2\boldsymbol{\sigma}_d \boldsymbol{\sigma}_d^T \} \quad (11)$$

Iterating using an initial state estimate and using Eq. 6 until the cost in Eq. 5 converges to a constant value provides a robust method for solving for the unknown locations and orientations of each detector with respect to the inertially-fixed calibration beacon cluster. Although there is no guarantee of convergence given for a significantly incorrect initial guess, in practice the algorithm typically converges within 4 iterations for this application even with initial position errors of 0.5m.

## B. GLSDC Algorithm Using Multiple Detectors

Once calibration is completed, the calibration beacon cluster is removed from the workspace, and the RMV takes its place. The RMV is triangular in shape and  $n_b$  beacons were placed on each side of the RMV, for a total of  $3n_b$  beacons. Following calibration, the Detector positions and orientations are known, and the position and orientation of the RMV become the unknowns. We assume perfect knowledge of the position of the beacons relative to the RMV frame, specified as vectors  $\mathbf{R}_i$ . Thus, the inertial position vector of each beacon is

$$\mathbf{X}_i = \mathbf{X}_r + [C(\boldsymbol{\sigma}_r)]^T \mathbf{R}_i \quad (12)$$

where  $\mathbf{X}_r$  is the unknown inertial position vector of the RMV and  $[C(\boldsymbol{\sigma}_r)]$  is the direction cosine matrix relating the inertial frame to the RMV frame as a function of the unknown RMV MRPs.

Again, GLSDC was used to compute the unknown 6-DOF state estimate,  $\mathbf{x}_r$  but the equations change slightly to allow for multiple detectors. In this case, the measurement model is replaced by

$$\hat{\mathbf{b}}_i = \mathbf{f}(\mathbf{x}_r) \quad (13)$$

$$= \frac{1}{r_i} [A] (\mathbf{X}_r + [C(\boldsymbol{\sigma}_r)]^T \mathbf{R}_i - \mathbf{X}_d) = \frac{1}{r_i} [A] \mathbf{r}_i \quad (14)$$

$$= \frac{1}{r_i} [A] (\mathbf{X}_r - \mathbf{X}_d) + \frac{1}{r_i} [A] [C(\boldsymbol{\sigma}_r)]^T \mathbf{R}_i \quad (15)$$

$$r_i = \|\mathbf{X}_r + [C(\boldsymbol{\sigma}_r)]^T \mathbf{R}_i - \mathbf{X}_d\| \quad (16)$$

The derivative with respect to the position simply changes sign, but the derivative with respect to MRPs changes significantly.

$$\frac{\partial \mathbf{f}}{\partial \mathbf{X}_r} = -\frac{1}{r_i} [A] (\hat{\mathbf{r}}_i \hat{\mathbf{r}}_i^T - [I_{3 \times 3}]) \quad (17)$$

$$\frac{\partial ([C]^T \mathbf{R}_i)}{\partial \boldsymbol{\sigma}_r} = \frac{4}{(1 + \boldsymbol{\sigma}_d^T \boldsymbol{\sigma}_d)^2} [[C]^T \mathbf{R}_i \times] \{ (1 - \boldsymbol{\sigma}_d^T \boldsymbol{\sigma}_d) [I_{3 \times 3}] + 2[\boldsymbol{\sigma}_d \times] + 2\boldsymbol{\sigma}_d \boldsymbol{\sigma}_d^T \} \quad (18)$$

$$\frac{\partial \mathbf{f}}{\partial \boldsymbol{\sigma}_r} = \frac{1}{r_i} [A] \frac{\partial ([C]^T \mathbf{R}_i)}{\partial \boldsymbol{\sigma}_r} - \frac{1}{r_i^2} \frac{\partial ([C]^T \mathbf{R}_i)}{\partial \boldsymbol{\sigma}_r} \mathbf{f} \quad (19)$$

Using these equations, a full 6-DOF state estimate of the RMV can be obtained at the update rate of the NorthStar Detector of 10Hz.

### C. Simulation Results

To test the above methods in simulation, we devised a reference scenario that consisted of Detectors placed around the perimeter of a 10m circular workspace. The Detectors were placed at a height of 2.4m and a distance of 13m from the center of the circle to reduce the probability of saturation when an RMV approached the edge of the workspace. The Detectors were aimed at the center of the workspace at the floor level. To test the calibration, the calibration beacon cluster was placed at the center of the circle. For testing of the localization system, three single OSRAM-LED beacons were placed half a meter apart on each side of the three-sided RMV. The reference height for the beacons was 0.3m off the floor, and the middle beacon on each side was raised by an additional 0.1m because decreased accuracy results from collinear beacons.

First, the calibration method was simulated using beacon cluster squares with side lengths of 0.5m, 1m, 1.5m, and 2m. The calibration routine was run 1000 times, and the standard deviation of the error was computed from these runs. The number of measurements was varied from a single measurement up to 100,000 (about 2.8hrs of calibration time at a 10Hz measurement rate), with the averaged value of the measurement set being used by the GLSDC algorithm. As expected by probability theory, the noise falls inversely proportional to the square root of the number of measurements. Also, as expected, larger beacon clusters resulted in lower calibration errors as shown in Fig. 7. Errors after 100,000 measurements reduced to less than 3mm position error and 1' attitude error in the 0.5m square case, and were reduced by a factor of 4 when a 2m square was used.

Next, the localization method was tested using from 1 to 6 Detectors spaced evenly around the perimeter of the circular workspace. The RMV was placed in the center of the workspace and Fig. 8 shows the 1- $\sigma$  position and angular accuracy for a single measurement as a function of the number of Detectors. Due to poor observability along the boresight of the Detector, both the 1 and 2 Detector cases have significant error along the x-axis, which dominates the total position error. Once a third Detector is introduced, that error drops to the same order of magnitude as the error in y. With three Detectors, position errors are below 3cm and the attitude error is below 3°. Adding additional detectors yields diminishing returns on accuracy, though larger numbers of Detectors improves line of sight issues when multiple RMVs are used.

To further characterize the localization accuracy, the RMV was moved throughout the workspace and the 1- $\sigma$  position errors computed assuming 4 Detectors are shown in Fig. 9. With 4 Detectors, accuracy better than  $\sim 5$ cm is achieved throughout the 20m diameter workspace. These results demonstrate the high accuracies possible with this method as a stand alone sensor, even at the large distances encountered in a 314m<sup>2</sup> workspace.

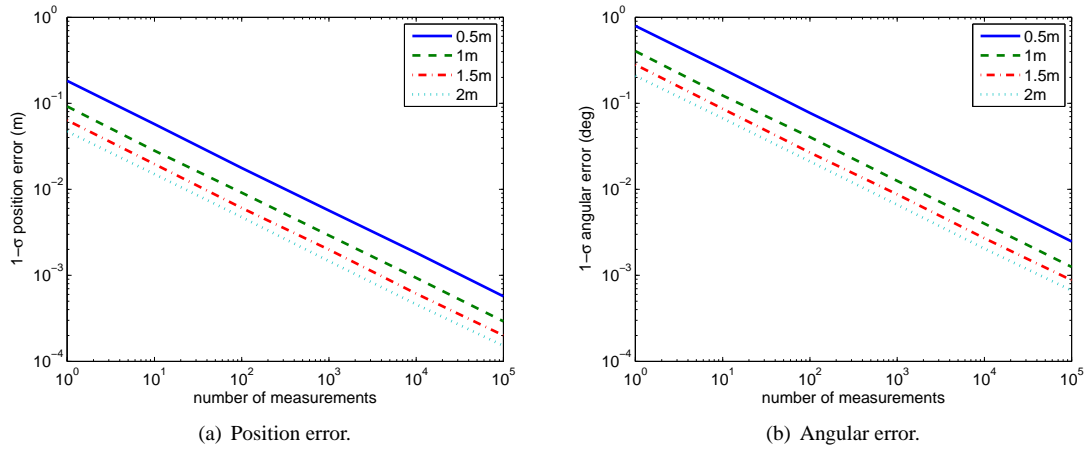


**Figure 7. 1- $\sigma$  standard deviation of Detector as a function of the number of measurements on a log-log scale. Each line corresponds to a different sized calibration square.**

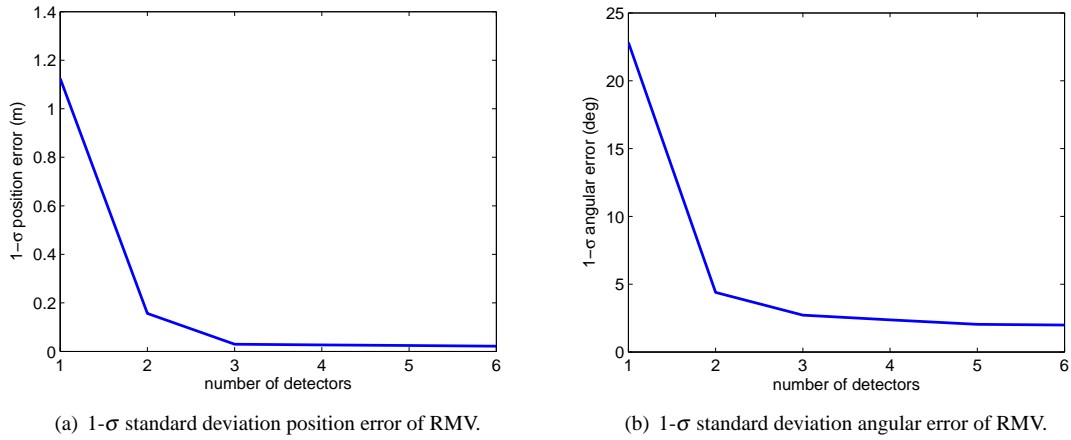


**Figure 8. State estimate error of the RMV as a function of the number of Detectors.**

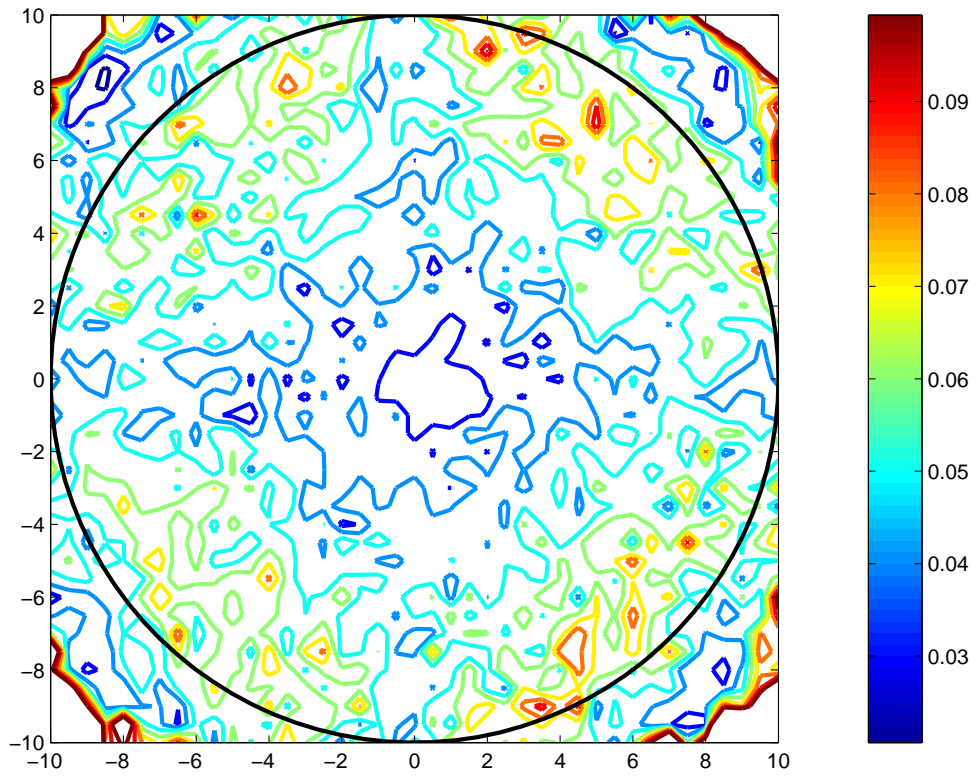


Figure 9. Contours represent 1- $\sigma$  position error throughout the workspace using 4 Detectors.

## V. Conclusion

We have used the direct beacon mode of the NorthStar system to produce a 6-D state estimate of our mobile robot. The formulation of the 6-DOF system is analogous to that of the VisNav relative navigation sensor. We note that whereas the methods described here are being applied to mobile robot localization, the same sensor system can be used as a relative position sensor in proximity operations.

The characterization of the NorthStar system provides important information for modeling and overall system design. Not only the distance between the beacons and the NorthStar Detector, but also the angles of each with respect to the line of sight play significant roles in the noise characteristics of the sensor. Further testing is needed to determine the relationship between beacon modulation frequency and the noise characteristics of the Detector, as the NorthStar documentation indicates two beacons operating at different frequencies may not yield equal intensity measurements. This finding was confirmed in hardware, but the relationship between frequency or number of beacons within view and intensity or noise has yet to be determined.

The simulation results demonstrate not only the accuracy of the system, but also that the NorthStar system can be effectively used as a 6-DOF measurement system. Combined with internal sensing measurement updates through a Kalman filter, this method promises even greater accuracy throughout the entire workspace.

## References

- <sup>1</sup>Creamer, G., Pipitone, F., Gilbreath, C., Bird, D., , and Hollander, S., "NRL Technologies for Autonomous Inter-Spacecraft Rendezvous and Proximity Operations," *Proceedings of the John L. Junkins Astrodynamics Symposium, AAS/AIAA Space Flight Mechanics Meeting*, College Station, Texas, May 2003.
- <sup>2</sup>Roe, F. D., Mitchell, D. W., Linner, B. M., and Kelley, D. L., "Simulation Techniques for Avionics Systems - An Introduction to a World Class Facility," *Proceedings of the AIAA Flight Simulation Technologies Conference*, San Diego, California, July 1996.
- <sup>3</sup>Davis, J. J., Doebbler, J., Dougherty, K., Junkins, J. L., and Valasek, J., "Aerospace Vehicle Motion Emulation Using Omni-directional Mobile Platform," *Proceedings of AIAA Guidance, Navigation, and Control Conference*, Hilton Head, SC, Aug 2007.
- <sup>4</sup>Doebbler, J., Davis, J. J., Valasek, J., and Junkins, J. L., "Odometry and Calibration Methods for Multi-Castor Vehicles," *IEEE International Conference on Robotics and Automation*, Pasadena, CA, May 2008.
- <sup>5</sup>Bai, X., Davis, J. J., Doebbler, J., Turner, J., and Junkins, J. L., "Dynamics, Control and Simulation of a Mobile Robotics System for 6-DOF Motion Emulation," *World Congress on Engineering and Computer Science*, San Francisco, CA, Oct 2007.
- <sup>6</sup>Evolution Robotics, Inc., *NorthStar Detector Kit: User Guide*, Part number: B-M-0059, Available internet <<http://www.evolution.com/products/northstar/>>.
- <sup>7</sup>Evolution Robotics, Inc., *NorthStar Projector Kit: User Guide*, Part number: B-M-0060, Available internet <<http://www.evolution.com/products/northstar/>>.
- <sup>8</sup>Evolution Robotics, Inc., *NorthStar Localization Detector: Product Data Specification (Data Sheet)*, Part number: 02-014-0045, Available internet <<http://www.evolution.com/products/northstar/>>.
- <sup>9</sup>Valasek, J., Gunnam, K., Kimmet, J., Tandale, M., Junkins, J., and Hughes, D., "Vision-Based Sensor and Navigation System for Autonomous Air Refueling," *AIAA Journal of Guidance, Control, and Dynamics*, Vol. 28, No. 5, Sept-Oct 2005, pp. 979-989.
- <sup>10</sup>Gunnam, K. K., Hughes, D. C., Junkins, J. L., and Kehtarnavaz, N., "A Vision-Based DSP Embedded Navigation Sensor," *IEEE Sensors Journal*, Vol. 2, No. 5, October 2002, pp. 428-442.
- <sup>11</sup>Du, J.-Y., *Vision Based Navigation System for Autonomous Proximity Operations: And Experimental and Analytical Study*, Ph.D. thesis, Aerospace Engineering Dept, Texas A&M University, December 2004.
- <sup>12</sup>Vishay Semiconductors, *TSAL7200 Datasheet*, November 2006, Document number 81012, Available internet <<http://www.vishay.com/docs/81012/tsal7200.pdf>>.
- <sup>13</sup>OSRAM Opto Semiconductors, *SFH 4231 Datasheet*, Available internet <<http://catalog.osram-os.com>>.
- <sup>14</sup>Schaub, H. and Junkins, J. L., *Analytical Mechanics of Space Systems*, AIAA Education Series, Reston, VA, 2003.
- <sup>15</sup>Crassidis, J. L. and Junkins, J. L., *Optimal Estimation of Dynamic Systems*, Chapman & Hall/CRC, New York, 2004.